

ORIGINAL ARTICLE

Water-soluble complexes formed from hydrogen bonding interactions between a poly(ethylene glycol)-containing triblock copolymer and poly(methacrylic acid)

Yuuichi Yokoyama^{1,2} and Shin-ichi Yusa¹

Poly(sodium styrenesulfonate)-*block*-poly(ethylene glycol)-*block*-poly(sodium styrenesulfonate) (PSS-PEG-PSS) was prepared via reversible addition-fragmentation chain transfer (RAFT) radical polymerization of sodium styrenesulfonate (SS) using a poly(ethylene glycol) (PEG)-based bifunctional macro-chain transfer agent in water. The reaction proceeded in the manner of living polymerization, suggesting that the number-average molecular weight increased linearly with monomer conversion, whereas the molecular weight distribution remained nearly constant below 1.30, independent of conversion. Poly(methacrylic acid) (PMA) homopolymer was also prepared via RAFT. When aqueous solutions of PSS-PEG-PSS and PMA were mixed below pH 5, water-soluble PSS-PEG-PSS/PMA complexes were formed as a result of hydrogen bonding interactions between the PEG block and the pendant carboxylic acids in PMA. The complex was characterized by ¹H NMR spin-spin relaxation time, light scattering and transmission electron microscopy measurement techniques. The hydrodynamic radius (R_h) of the complex depended on the mixing ratio of the PSS-PEG-PSS and PMA molecules. When the mole ratio of ethylene glycol units in PSS-PEG-PSS and the pendant carboxylic acids in PMA was nearly unity, the scattering intensity and R_h exhibited maximum values for PSS-PEG-PSS and PMA, which is indicative of stoichiometric complex formation. The complex dissociated at pH greater than 5 because the hydrogen bonding interaction ceased as a result of deprotonation of the pendant carboxylic acids in PMA.

Polymer Journal (2013) 45, 985–992; doi:10.1038/pj.2013.2; published online 20 February 2013

Keywords: block copolymer; hydrogen bond; poly(ethylene glycol); reversible addition-fragmentation chain transfer radical polymerization; water-soluble complex

INTRODUCTION

Complex formation between polymers can be driven by non-covalent interactions, including hydrophobic,¹ electrostatic,^{2,3} Van der Waals⁴ and hydrogen bonding interactions.^{5,6} Hydrogen bonding interactions, in particular, are an important driving force for self-organization of natural polymers such as proteins, polysaccharides and DNA.

It is known that poly(ethylene glycol) (PEG) and poly(methacrylic acid) (PMA) form a water-insoluble complex in water owing to hydrogen bonding interactions between the ethylene glycol groups in PEG and the pendant carboxylic acid groups in PMA.^{7,8} In these interactions, the ethylene glycol repeat units in PEG and the pendant carboxylic acids in PMA act as hydrogen acceptors and donors, respectively. Generally, the interaction between ethylene glycol and carboxylic acid groups is weak, but the interaction between PEG and PMA is strong owing to multiple hydrogen bonding interactions. The water-insoluble complex dissociates under basic conditions

because the hydrogen bonding interactions disappear as a result of deprotonation of the pendant carboxylic acids in PMA.⁹ Holappa *et al.*¹⁰ reported the self-complexation of poly(ethylene glycol)-*block*-poly(methacrylic acid). This self-complexation was studied as a function of the degree of ionization using fluorescence techniques. Below a pH of 4.5, poly(ethylene glycol)-*block*-poly(methacrylic acid) formed intermolecular aggregates; within the pH range of 4.5–5.5, intramolecular hydrogen bonding governed the conformation of the block copolymers; and above a pH of 6.0, the block copolymers adopted an open-coil conformation typical of polyelectrolytes. Van Hest *et al.*¹¹ reported that block copolymer assemblies were formed between nucleobase-functionalized block copolymers prepared via atom transfer radical polymerization from a PEG-based macroinitiator of either thymine- or adenine-functionalized methacrylates. Hydrogen bonding interactions between the thymine and adenine moieties have a crucial role in the aggregation behavior of block copolymers.

¹Department of Materials Science and Chemistry, University of Hyogo, Himeji, Japan and ²Medical Material Department, R&D Division, Taki Chemical Co., Ltd., Kakogawa, Japan

Correspondence: Dr S-i Yusa, Department of Materials Science and Chemistry, University of Hyogo, 2167 Shosha, Himeji, Hyogo 671-2280, Japan.

E-mail: yusa@eng.u-hyogo.ac.jp

Received 19 November 2012; revised 10 December 2012; accepted 16 December 2012; published online 20 February 2013

The recent development of controlled radical polymerization has provided a useful tool for the synthesis of various types of block copolymers with controlled structures. In particular, reversible addition-fragmentation chain transfer (RAFT) radical polymerization offers certain advantages because it is a metal-free method. For example, water-soluble polyelectrolytes can be easily prepared via RAFT-controlled radical polymerization.^{12–14}

Self-assembly of PEG-based block copolymers and PMA homopolymers owing to hydrogen bonding interactions has not previously been reported. In this study, an ABA triblock copolymer (PSS–PEG–PSS) composed of poly(sodium styrenesulfonate) (PSS) and PEG blocks was prepared via RAFT radical polymerization (Figure 1). A PMA homopolymer was also prepared via RAFT. When the PSS–PEG–PSS and PMA polymers were mixed in water, a water-soluble PSS–PEG–PSS/PMA complex was formed through hydrogen bonding interactions between the PEG block and PMA at pH 3. The complex dissociated under basic conditions when the hydrogen bonding interactions disappeared as a result of deprotonation of the pendant carboxylic acids in PMA.

EXPERIMENTAL PROCEDURE

Materials

Methacrylic acid (MA) from Kanto Chemical (Tokyo, Japan) was dried over 4 Å molecular sieves and distilled under reduced pressure. 4-Cyanopentanoic acid dithiobenzoate (CPD) was synthesized according to the method reported by McCormick and coworkers.¹⁵ Dichloromethane, chloroform and methanol from Kanto Chemical and tetrahydrofuran from Wako Pure Chemical Industries (Osaka, Japan) were dried over 4 Å molecular sieves and distilled. SS (>93%) from Tokyo Chemical Industry (Tokyo, Japan), α,ω -bis-hydroxy poly(ethylene glycol) (HO-PEG-OH, number-average molecular weight (M_n) = 1.00×10^4 , number-average degree of polymerization (DP) = 227) and 8-anilino-1-naphthalenesulfonic acid ammonium salt hydrate (ANS, $\geq 97\%$) from Sigma Aldrich (St Louis, MO, USA), N,N' -dicyclohexylcarbodiimide (99%) from Kishida Chemical (Osaka, Japan), and 4-(dimethylamino) pyridine (99%) and 4,4'-azobis(4-cyanopentanoic acid) (V-501, 98%) from Wako Pure Chemical Industries were used as received without further purification. Water was purified using a Millipore (Billerica, MA, USA) Milli-Q system. Other reagents were used as received.

Synthesis of the PEG-based bifunctional chain transfer agent (CPD-PEG-CPD)

A PEG-based bifunctional chain transfer agent (CPD-PEG-CPD) was synthesized according to the literature, with slight modifications.¹⁶ A dichloromethane solution (100 ml) of N,N' -dicyclohexylcarbodiimide (3.15 g, 15.3 mmol) was added dropwise to a dichloromethane solution (150 ml) of HO-PEG-OH ($M_n = 1.00 \times 10^4$, 50.1 g, 5.01 mmol), CPD (3.38 g, 12.1 mmol) and a trace of 4-(dimethylamino) pyridine over a period of 30 min. After being stirred for 20 h at 40 °C, the reaction mixture was filtrated to remove dicyclohexylurea. The solvent was removed, and the crude product was purified by silica gel chromatography using a mixture of chloroform and methanol (90:10 v/v) as the eluent, affording CPD-PEG-CPD as a red powder (42.2 g, 79.0%). The values of M_n and the molecular weight distribution (M_w/M_n) were estimated by gel-permeation chromatography (GPC) to be 1.00×10^4 and 1.18, respectively.

Preparation of the poly(sodium styrenesulfonate)-block-poly(ethylene glycol)-block-poly(sodium styrenesulfonate) triblock copolymer (PSS–PEG–PSS)

SS (1.45 g, 7.01 mmol), V-501 (7.81 mg, 0.0279 mmol) and CPD-PEG-CPD (0.74 g, 0.07 mmol) were dissolved in water (40.0 ml). The mixture was degassed by purging with Ar gas for 30 min. Polymerization was carried out at 70 °C for 5 h, after which the polymerization mixture was poured into a large excess of tetrahydrofuran to precipitate the resulting polymer, which was dialyzed against pure water for 1 day. The triblock copolymer (PSS–PEG–PSS) was recovered by a freeze-drying technique (1.50 g, 68.3%). The values of M_n and M_w/M_n were estimated by GPC to be 1.88×10^4 and 1.24, respectively. The DP of one PSS block was 39, estimated by ^1H NMR.

To investigate the relationship between the polymerization time and the extent of conversion, the conversion was determined by ^1H NMR spectroscopy. Predetermined amounts of SS (0.311 g, 1.51 mmol), CPD-PEG-CPD (0.159 g, 0.015 mmol) and V-501 (0.002 g, 0.006 mmol) were dissolved in 8.86 ml of D_2O . The solution was transferred to several NMR tubes and degassed by purging with Ar gas for 30 min. The cap was sealed, and the solution was heated to 70 °C in a preheated oil bath for varying lengths of time. Polymerization was terminated by rapid cooling in an ice bath. The monomer conversion, estimated by ^1H NMR, was monitored as a function of reaction time. GPC measurements were obtained for the reaction mixture to estimate M_n and M_w/M_n .

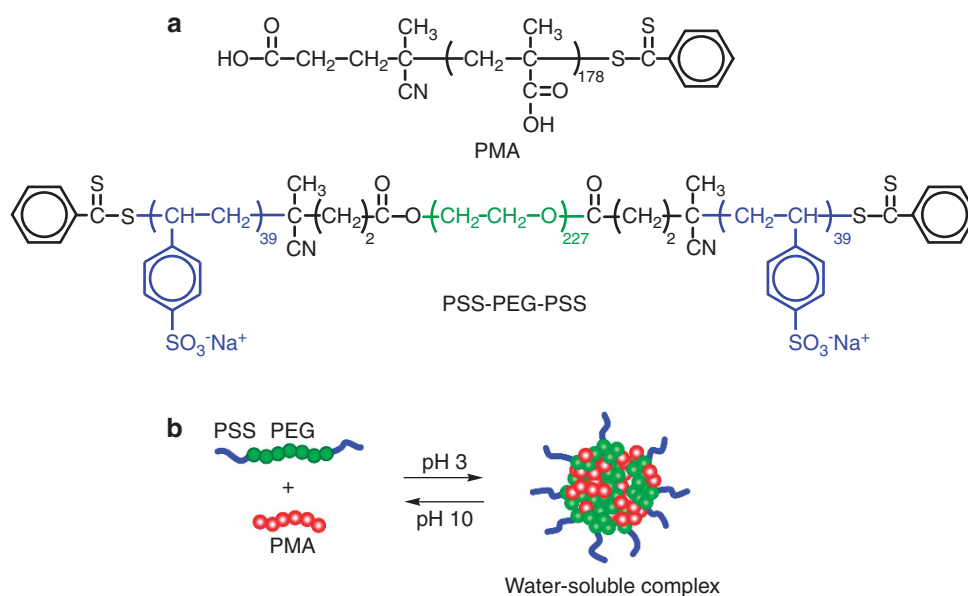


Figure 1 (a) Chemical structures of PSS–PEG–PSS and PMA. (b) Schematic representation of the water-soluble complex formation between PSS–PEG–PSS and PMA.

Preparation of PMA

PMA was synthesized according to the literature, with modifications.¹⁷ MA (10.3 g, 120 mmol), V-501 (51.9 mg, 0.185 mmol) and CPD (0.26 g, 0.922 mmol) were dissolved in water (110 ml). The mixture was degassed by purging with Ar gas for 30 min, followed by polymerization at 80 °C for 4 h. The polymerization mixture was dialyzed against pure water for 1 week. The homopolymer (PMA) was recovered by a freeze-drying technique (9.81 g, 92.9%). The M_n and M_w/M_n values, determined by ¹H NMR and GPC, were 1.56×10^4 and 1.14, respectively. The DP value for the PMA block was 178, as estimated by ¹H NMR.

Preparation of the water-soluble complex

PSS-PEG-PSS and PMA were separately dissolved in 0.1 M NaCl at pH 3. For preparation of the complex, the PSS-PEG-PSS solution was added to the PMA solution over a period of 5 min at room temperature while stirring, and the mixture was allowed to equilibrate for at least 1 day before measurement. The mixing ratio of the two polymers was adjusted based on the mole fraction of ethylene glycol units ($f_{EG} = [EG]/([MA] + [EG])$), where [EG] and [MA] are the mole concentrations of ethylene glycol and MA units, respectively. The water-soluble complex was prepared at $f_{EG} = 0.5$ unless otherwise noted.

Characterization

GPC measurements were performed using a Tosoh (Tokyo, Japan) DP-8020 pump and a Tosoh RI-8020 refractive index (RI) detector equipped with a Shodex (Tokyo, Japan) Asahipak 7.0- μ m bead size GF-7M HQ column (exclusion limit $\sim 10^7$) working at 40 °C with a flow rate of 0.6 ml min⁻¹. Sample solutions for the GPC measurements were filtered using a 0.2- μ m pore size membrane filter. A phosphate buffer (pH 9) containing 10 vol% acetonitrile was used as an eluent at a flow rate of 0.6 ml min⁻¹. The values of M_n and M_w/M_n for the polymers were calibrated using standard PSS samples of 11 different molecular weights ranging from 1.37×10^3 to 2.16×10^6 .

¹H NMR spectra were obtained using a Bruker BioSpin (Billerica, MA, USA) DRX-500 spectrometer operating at 500 MHz. ¹H NMR spin-spin relaxation times (T_2) were determined by the Carr-Purcell-Meiboom-Gill method.^{18,19} For T_2 measurements, sample solutions of the polymer were prepared in D₂O containing 0.1 M NaCl with a polymer concentration (C_p) of 0.83 g l⁻¹. NMR tubes containing the D₂O solution were deaerated by purging with Ar gas for 30 min. A 90° pulse of 13.85 μ s duration was calibrated and used for the measurements.

Light scattering measurements were performed using an Otsuka Electronics Photal (Osaka, Japan) DLS-7000HL light scattering spectrometer equipped with an ALV (Langen, Germany) 5000E multi- τ digital time correlator. A He-Ne laser (10.0 mW at 632.8 nm) was used as a light source. Sample solutions for the light scattering measurements were filtered using a 0.2- μ m pore size membrane filter.

In static light scattering measurements, the weight-average molecular weight (M_w), z-average radius of gyration (R_g) and second virial coefficient (A_2) values were estimated from the relation

$$\frac{KC_p}{R_\theta} = \frac{1}{M_w} \left(1 + \frac{1}{3} R_g^2 q^2 \right) + 2A_2 C_p \quad (1)$$

where R_θ is the difference between the Rayleigh ratio of the solution and that of the solvent, $K = 4\pi^2 n^2 (dn/dC_p)^2 / N_A \lambda^4$ with dn/dC_p representing the RI increment against C_p , N_A is Avogadro's number and q is the magnitude of the scattering vector. The q value is calculated from $q = (4\pi n/\lambda) (\sin(\theta/2))$, where n is the RI of the solvent, λ is the wavelength of light source (632.8 nm) and θ is the scattering angle. The known Rayleigh ratio of toluene was used to calibrate the instrument. Values of dn/dC_p at 633 nm were determined using an Otsuka Electronics Photal DRM-3000 differential refractometer.

To obtain the relaxation time distribution $\tau A(\tau)$ from the dynamic light scattering (DLS) measurements, an inverse Laplace transform analysis was performed using the REPES algorithm.^{20–22} The relaxation rate ($\Gamma = \tau^{-1}$) is a function of θ .²³ The diffusion coefficient (D) is calculated from $D = (\Gamma/q^2)_{q \rightarrow 0}$. The hydrodynamic radius (R_h) is given by the Stokes-Einstein equation,

$R_h = k_B T / (6\pi\eta D)$, where k_B is the Boltzmann constant, T is the absolute temperature and η is the solvent viscosity. The details of the DLS instrumentation and theory are described in the literature.^{24–26}

Fluorescence spectra were recorded using a Hitachi (Tokyo, Japan) F-2500 fluorescence spectrophotometer. A stock solution of 0.02 mM ANS in aqueous 0.1 M NaCl was prepared. Fluorescence emission spectra of ANS were measured with excitation at 350 nm. The slit widths for the excitation and emission sides were kept at 20 and 5.0 nm, respectively, during measurement.

Transmission electron microscopy (TEM) observations were carried out with a JEOL (Tokyo, Japan) JEM-2100 microscope at an accelerating voltage of 200 kV. Samples for TEM observations were prepared by placing one drop of aqueous solution on a copper grid coated with thin films of Formvar and carbon. Excess water was blotted using a filter paper. The samples were stained with sodium phosphotungstate and dried under vacuum for 1 day.

RESULTS AND DISCUSSION

We performed RAFT radical polymerization of SS using CPD-PEG-CPD ($M_n = 1.00 \times 10^4$, $M_w/M_n = 1.18$). The polymerization of SS using CPD-PEG-CPD proceeded in a controlled manner as illustrated in Figure 2. In Figure 2a, a time-conversion relationship is depicted along with the first-order kinetic plot for the polymerization of SS in the presence of CPD-PEG-CPD at 70 °C in D₂O under an Ar atmosphere. The monomer consumption was monitored by ¹H NMR spectroscopy as a function of the polymerization time. There was an induction period of ~ 84 min, which may be owing to the slow rate of formation of the 4-cyanopentanoic acid radical fragment, as reported by McCormick and coworkers.²⁷ A monomer conversion level of 98.2% was reached within 6 h. The kinetics plot for the RAFT polymerization of SS, shown in Figure 2a, indicates that the concentration of the propagating radical remained constant during the polymerization.

Figure 2b shows GPC elution curves for the polymerization of SS in the presence of CPD-PEG-CPD. A significant increase in molecular weight occurred upon the polymerization of SS, indicating the formation of the block copolymer PSS-PEG-PSS. Neither a new peak nor a shoulder owing to the presence of PSS homopolymers was observed. Thus, it was concluded that no concurrent homopolymerization of SS occurred.

In Figure 2c, values of M_n and M_w/M_n for the triblock copolymer PSS-PEG-PSS, estimated from GPC measurements, are plotted as a function of the extent of SS conversion. The M_n value increased with the conversion, whereas M_w/M_n remained in a somewhat narrow range of 1.07–1.27, independent of conversion. The polymerization of PMA in the presence of CPD also proceeded in a controlled manner, with a narrow M_w/M_n value (1.14).¹⁷

Figure 3 shows ¹H NMR spectra of PSS-PEG-PSS, PMA and the PSS-PEG-PSS/PMA complex in D₂O containing 0.1 M NaCl at pH 3. In the spectrum of PSS-PEG-PSS, the resonance band observed at 0.9–2.3 p.p.m. was attributed to the main chain protons of the PSS blocks. The DP of the PSS blocks in PSS-PEG-PSS and the M_n (NMR) for PSS-PEG-PSS were determined from the intensity ratio of the resonance bands owing to the pendant phenyl protons in the PSS block at 6.1–7.9 p.p.m. and the PEG main chain protons at 3.7 p.p.m. As shown in Figure 3b, the resonance bands observed in the 0.6–2.8 p.p.m. region in the PMA spectrum were attributed to the α -methyl protons and main chain methylene protons, respectively. The DP and M_n (NMR) of PMA were determined based on the intensity ratio of the resonance bands owing to the terminal phenyl protons at 7.5–8.4 p.p.m. and the PMA main chain protons at 0.6–2.8 p.p.m.

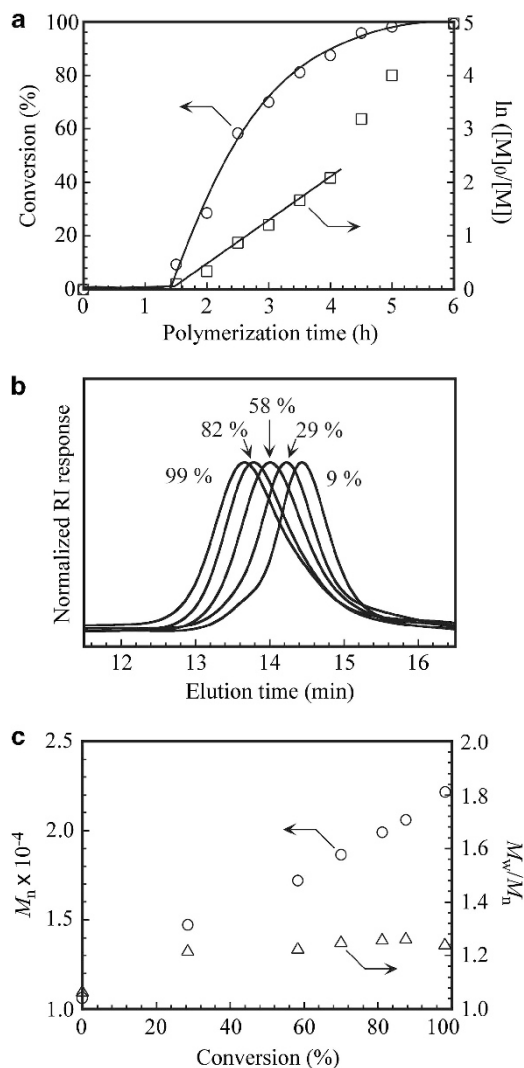


Figure 2 (a) Time-conversion (○) and first-order kinetic plots (□) for the polymerization of SS in the presence of CPD-PEG-CPD in water at 70 °C. $[M]_0$ and $[M]$ represent the concentrations of the monomer at a polymerization time of 0 and the corresponding time, respectively. (b) GPC elution curves demonstrating the evolution of the molecular weight during the polymerization of SS using CPD-PEG-CPD. Conversions are shown for each peak. (c) Dependence of M_n (○) and M_w/M_n (Δ) on monomer conversion in the polymerization of SS in the presence of CPD-PEG-CPD.

If polymerization is assumed to be ideally living in nature, then the theoretical number-average molecular weight ($M_n(\text{theo})$) can be calculated as

$$M_n(\text{theo}) = \frac{[M]_0}{[CTA]_0} \frac{x_m}{100} M_m + M_{CTA} \quad (2)$$

where $[M]_0$ is the initial monomer concentration, $[CTA]_0$ is the initial CPD-PEG-CPD concentration, x_m is the percentage conversion of the monomer, M_m is the molecular weight of the monomer and M_{CTA} is the molecular weight of CPD-PEG-CPD. The $M_n(\text{NMR})$ values for PSS-PEG-PSS and PMA were calculated from the ^1H NMR data. As shown in Table 1, the $M_n(\text{NMR})$ value for PSS-PEG-PSS was in reasonable agreement with $M_n(\text{theo})$. However, the $M_n(\text{theo})$ and $M_n(\text{GPC})$ values for PSS-PEG-PSS were slightly different because PSS was used as a standard polymer to calibrate $M_n(\text{GPC})$, and its volume-

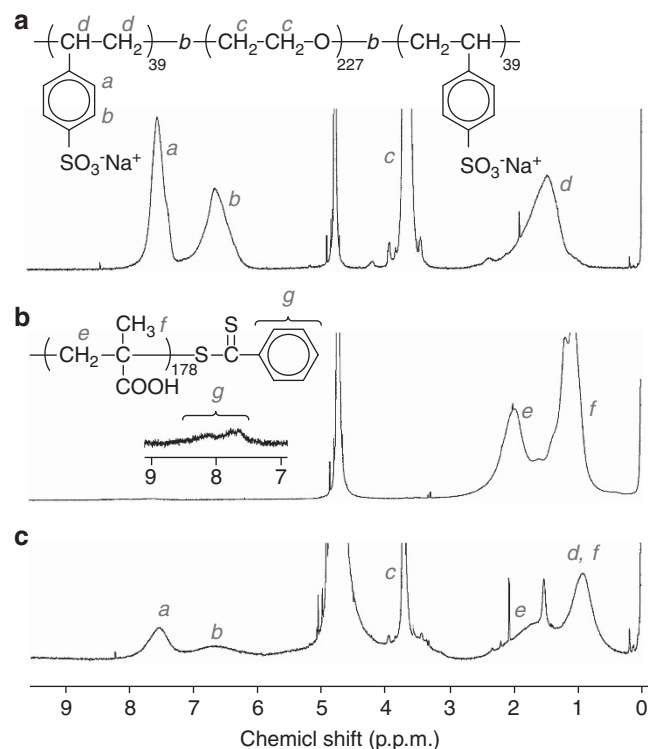


Figure 3 ^1H NMR spectra measured in D_2O containing 0.1 M NaCl at pH 3 for (a) PSS-PEG-PSS, (b) PMA and (c) the PSS-PEG-PSS/PMA complex. Assignments are indicated for the resonance peaks. A full color version of this figure is available at *Polymer Journal* online.

Table 1 Number-average molecular weights (M_n) and molecular weight distributions (M_w/M_n) of the polymers

Sample	$M_n(\text{theo})^a$ $\times 10^{-4}$	$M_n(\text{NMR})^b$ $\times 10^{-4}$	$M_n(\text{GPC})^c$ $\times 10^{-4}$	M_w/M_n^c
PSS-PEG-PSS	2.94	2.66	1.88	1.24
PMA	1.44	1.95	2.16	1.14

Abbreviations: $M_n(\text{GPC})$, M_n estimated from gel-permeation chromatography (GPC); $M_n(\text{NMR})$, M_n estimated from ^1H NMR; $M_n(\text{theo})$, theoretical M_n ; PMA, poly(methacrylic acid); PSS-PEG-PSS, poly(sodium styrenesulfonate)-*block*-poly(ethylene glycol)-*block*-poly(sodium styrenesulfonate).

^aCalculated from equation (2).

^bEstimated from ^1H NMR.

^cEstimated from GPC.

to-mass ratio may be different from that of PSS-PEG-PSS.^{28,29} The $M_n(\text{NMR})$ value for PMA was relatively close to the $M_n(\text{theo})$ value.

Figure 3c shows the ^1H NMR spectrum of a mixture of PSS-PEG-PSS and PMA prepared in D_2O containing 0.1 M NaCl at pH 3. The PSS-PEG-PSS/PMA complex was expected to form a core-shell micelle structure in which the complexed PEG/PMA blocks formed the core, with the PSS blocks surrounding the core to form the shell layer. To obtain further information about motional restriction of the PEG blocks, ^1H NMR spin-spin relaxation times (T_2) were measured for PSS-PEG-PSS and the PSS-PEG-PSS/PMA complex; a decrease in T_2 suggests restricted motion of the protons.^{30,31} The T_2 value at 3.7 p.p.m. for the PEG protons in PSS-PEG-PSS before mixing with PMA was 160 ms, while the T_2 for the PEG protons in the complex was shorter ($T_2 = 41.5$ ms). This observation indicates restricted motion of the PEG blocks in the complex owing to hydrogen bonding between the PEG block and PMA.

Figure 4 shows the hydrodynamic radii (R_h) and light scattering intensities for a mixture of PSS–PEG–PSS and PMA in 0.1 M NaCl at pH 3 as a function of f_{EG} . The total C_p was kept constant at 0.83 g l^{-1} . An increase in the scattering intensity indicates an increase in the size of the complex. Maximum R_h and scattering intensity were observed at $f_{EG} = 0.5$. These results indicate that a stoichiometric interaction in the mixture of PSS–PEG–PSS and PMA led to the formation of the complex with maximum aggregation number. The complex with $f_{EG} = 0.5$ was used for this study, unless otherwise stated.

Figure 5 shows R_h distributions for the polymers at pH 3 and the PSS–PEG–PSS/PMA complex at pH 3 and 10. The values of R_h were determined by DLS in 0.1 M NaCl; these are shown in Table 2. The R_h values for PSS–PEG–PSS and PMA were 4.9 and 4.7 nm, respectively, which are reasonable for a unimer state. The R_h values of the complex at pH 3 and 10 were 43.4 and 4.8 nm, respectively. It was concluded that when PSS–PEG–PSS and PMA are mixed in 0.1 M NaCl at pH 3,

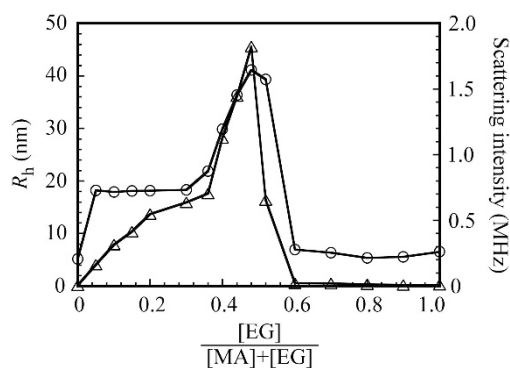


Figure 4 Hydrodynamic radii (R_h) (\circ) and light scattering intensities (Δ) of PSS–PEG–PSS/PMA complexes as a function of f_{EG} ($[EG]/([MA]+[EG])$) in 0.1 M NaCl aqueous solutions at pH 3. The total polymer concentration was fixed at 0.83 g l^{-1} . $[EG]$ and $[MA]$ represent the concentrations of the ethylene glycol and MA units, respectively.

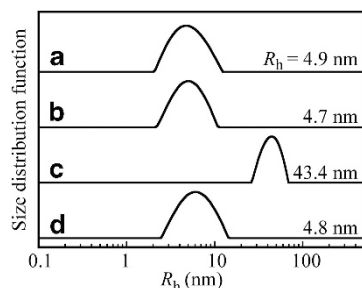


Figure 5 R_h distributions for (a) PSS–PEG–PSS and (b) PMA in 0.1 M NaCl at pH 3, and PSS–PEG–PSS/PMA complex at (c) pH 3 and (d) pH 10.

Table 2 Light scattering data for PSS–PEG–PSS, PMA and the PSS–PEG–PSS/PMA complex at pH 3

Samples	$M_w \times 10^{-4}$ (SLS)	R_g (nm)	R_h (nm)	R_g/R_h	N_{agg}
PSS–PEG–PSS	2.77	12.5	4.9	2.55	1
PMA	1.42	8.93	4.7	1.90	1
PSS–PEG–PSS/PMA complex	566	30.4	43.4	0.72	270

Abbreviations: M_w , weight-average molecular weight; N_{agg} , aggregation number; PMA, poly(methacrylic acid); PSS–PEG–PSS, poly(sodium styrenesulfonate)-*block*-poly(ethylene glycol)-*block*-poly(sodium styrenesulfonate); R_g , radius of gyration; R_h , hydrodynamic radius; SLS, static light scattering.

a water-soluble complex is formed by hydrogen bonding interactions between the PEG block and PMA, and this complex dissociates at pH 10 because the hydrogen bonding interaction disappears as a result of deprotonation of the pendant carboxylic acids in PMA.

The relaxation rates (Γ) measured at different scattering angles (θ) were plotted as a function of the square of the magnitude of the scattering vector (q^2) in Figure 6a. A linear relation passing through the origin indicates that the relaxation modes are virtually diffusive.³² The R_h value of 42.9 nm, estimated from the slope of the Γ versus q^2 plot, was found to be in good agreement with the R_h value (43.4 nm) calculated from the peak of the R_h distribution obtained at $\theta = 90^\circ$ (Figure 5c). As the angular dependence was negligible, the R_h values were estimated at a fixed θ of 90° . In Figure 6b, R_h is plotted against C_p . The R_h values for the complex were practically constant ($R_h =$ approximately 42 nm) in the C_p range from 0.17 to 0.83 g l^{-1} .

Figure 7a shows the light scattering intensities of 0.1 M NaCl aqueous solutions of the PSS–PEG–PSS/PMA complex plotted against C_p . The intensity increased sharply with increasing C_p above a threshold of 0.057 g l^{-1} . This observation suggests that the formation of a complex between PSS–PEG–PSS and PMA started to occur above a C_p of 0.057 g l^{-1} . The apparent critical aggregate concentration (CAC) value for the complex, estimated from the plot, was 0.057 g l^{-1} .

ANS is commonly used as a fluorescence probe to investigate molecular assemblies of surfactants and amphiphilic polymers because the fluorescence intensity of ANS increases in hydrophobic environments.³³ In Figure 7b, the fluorescence intensity of ANS in the presence of the PSS–PEG–PSS/PMA complex is plotted as a function

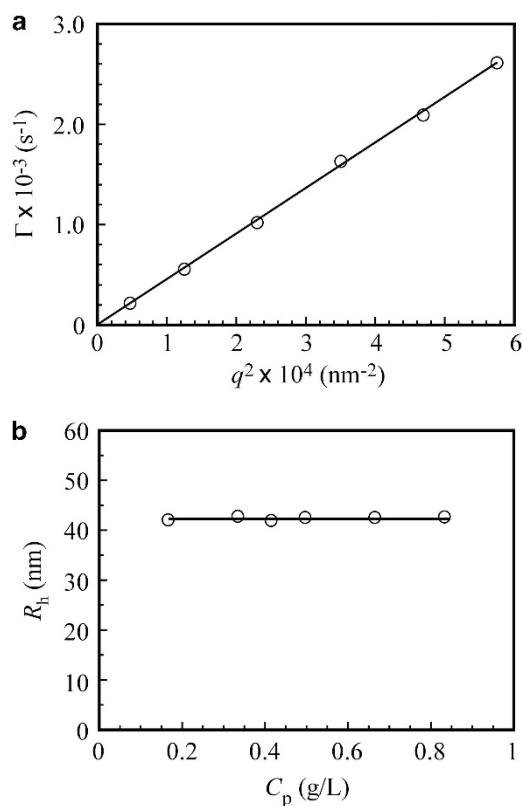


Figure 6 (a) Relationship between the relaxation rate (Γ) and the square of the magnitude of the scattering vector (q^2) for the PSS–PEG–PSS/PMA complex at $C_p = 0.83 \text{ g l}^{-1}$ in 0.1 M NaCl at pH 3. (b) R_h for the complex as a function of C_p in 0.1 M NaCl at pH 3.

of C_p . The intensity increased gradually in the lower C_p region, but began to increase more steeply at C_p values above 0.058 g l^{-1} . This increase indicates the existence of hydrophobic microdomains formed by hydrogen bonding interactions between the PEG block and PMA. The apparent CAC value for the complex was estimated graphically as 0.058 g l^{-1} ; the apparent CAC value based on the ANS fluorescence measurements was fairly close to that estimated from the light scattering data.

The apparent values of M_w and R_g , determined by static light scattering measurements, are listed in Table 2. Figure 8 shows Zimm plots for the PSS-PEG-PSS/PMA complex. The aggregation number (N_{agg}) for the complex, defined as the total number of polymer chains forming one complex, can be calculated from the ratio of the M_w values for the complex and the unimer. The result of this calculation gives an N_{agg} of 270 for the complex. The chain numbers of PSS-PEG-PSS and PMA for one complex were 119 and 151, respectively, as calculated from $f_{\text{EG}} = 0.5$ and the DP values of PEG and PMA.

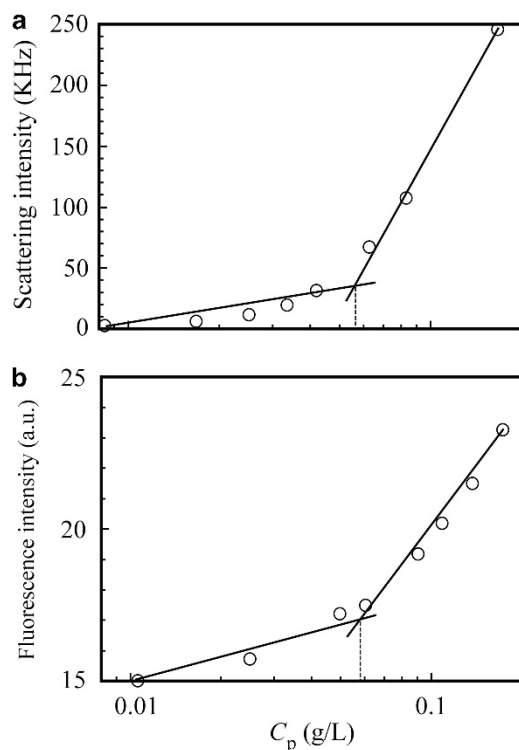


Figure 7 (a) Light scattering intensity of the PSS-PEG-PSS/PMA complex as a function of C_p in 0.1 M NaCl at pH 3. (b) Fluorescence intensity in ANS (0.02 mm) in the presence of the PSS-PEG-PSS/PMA complex as a function of C_p in 0.1 M NaCl at pH 3.

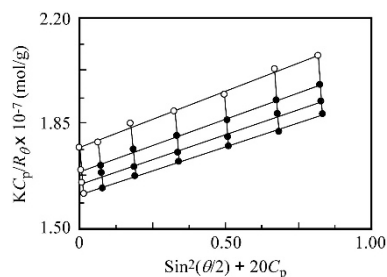


Figure 8 Zimm plots for the PSS-PEG-PSS/PMA complex in a 0.1 M NaCl aqueous solution at pH 3. Angles are from 30° to 130° in 20° increments.

The R_g/R_h value is useful for characterizing the shape of the molecular assemblies. The theoretical value of R_g/R_h for a homogeneous hard sphere is 0.778, but this value increases substantially for less dense structures and polydisperse mixtures; for example, $R_g/R_h = 1.5\text{--}1.7$ for flexible linear chains in good solvents, whereas $R_g/R_h \geq 2$ for a rigid rod.^{34–36} As shown in Table 2, the R_g/R_h ratio for the complex was found to be 0.72, which suggested that the shape of the complex was close to spherical. The R_g/R_h ratios for PSS-PEG-PSS and PMA were 2.55 and 1.90, respectively, which indicates that these polymers had relatively expanded conformations.

The core radius (R_{core}) of the PSS-PEG-PSS/PMA complex, based on a simple core-shell structure, can be calculated from the volume of each polymer as follows:

$$R_{\text{core}} = \left(\frac{3V_{\text{core}}}{4\pi} \right)^{1/3} = \left(\frac{3}{4\pi N_A} \left(\frac{M_{w,\text{PEG}}}{\rho_{\text{PEG}}} + \frac{M_{w,\text{PMA}}}{\rho_{\text{PMA}}} \right) \frac{N_{\text{agg}}}{2} \right)^{1/3} \quad (3)$$

where V_{core} is the core volume of the complex, $M_{w,\text{PEG}}$ and $M_{w,\text{PMA}}$ are the weight-average molecular weights of the PEG and PMA blocks, respectively, and ρ_{PEG} and ρ_{PMA} are the densities of the PEG block and PMA, respectively. From R_g and R_{core} , the shell thickness (L) can be calculated as $L = R_g - R_{\text{core}}$. For the calculation of R_{core} , the bulk densities of the EG and MA monomers were used ($\rho_{\text{PEG}} = 1.11$ and $\rho_{\text{PMA}} = 1.02 \text{ g cm}^{-3}$). Thus, values of R_{core} and L for the complex were calculated to be 20.8 and 9.6 nm, respectively. The contour

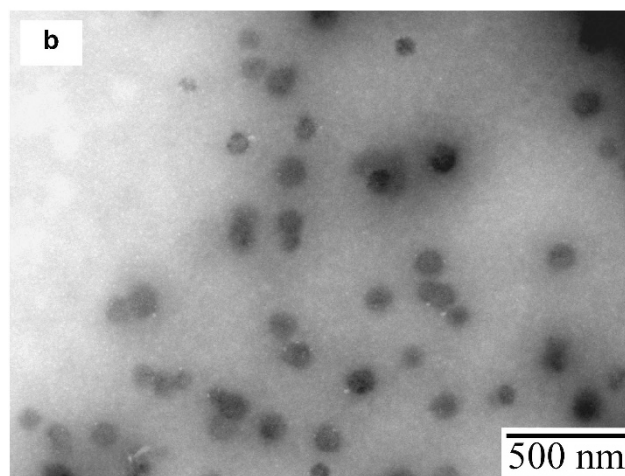
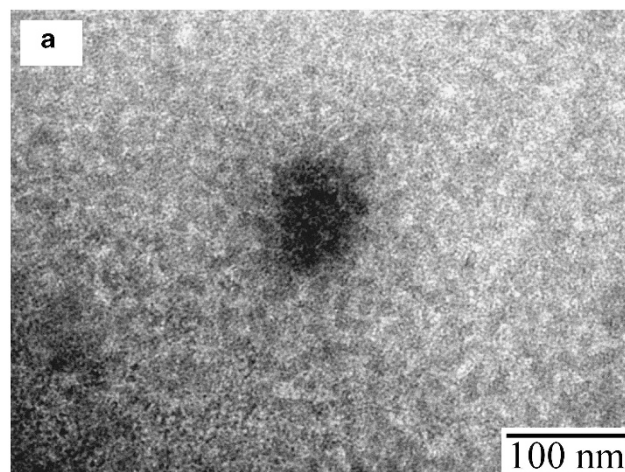


Figure 9 TEM images of the PSS-PEG-PSS/PMA complex. The scale bars are (a) 100 nm and (b) 500 nm.

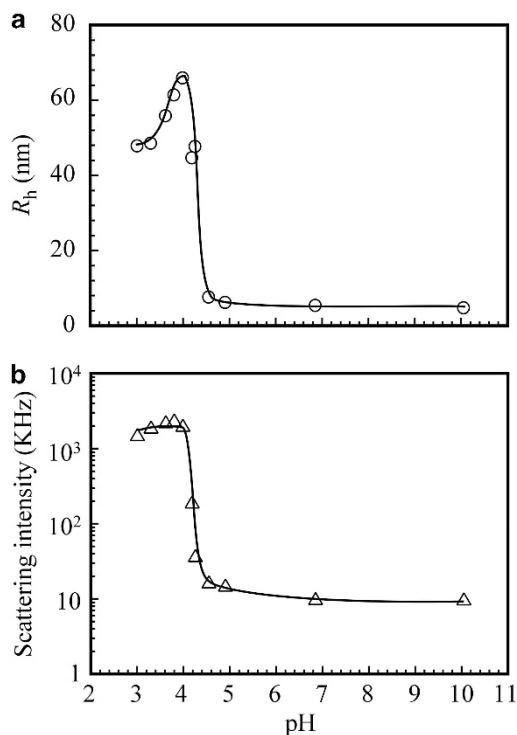


Figure 10 (a) R_h values and (b) scattering intensities for the PSS-PEG-PSS/PMA complex as a function of pH in 0.1 M NaCl.

length of PSS blocks with a DP of 39 can be calculated as 9.8 nm.^{37,38} The value of $L = 9.6$ nm for the complex is slightly smaller than the contour length of the PSS blocks. These results indicate that the complex was composed of a PEG/PMA core formed by hydrogen bonding interactions, with expanded PSS shells.

Figure 9 shows TEM images of the PSS-PEG-PSS/PMA complex. These show a spherical complex with an average diameter of 95 nm. The radius of the complex as observed by TEM was fairly close to the R_h value estimated by DLS.

Figure 10a shows R_h values for the PSS-PEG-PSS/PMA complex as a function of pH. Above a pH of 4.6, the R_h values were on the order of 5 nm, suggesting that PSS-PEG-PSS and PMA were in a unimer state. With decreasing pH, R_h started to increase around pH 4.5, reaching a maximum value of 65.9 nm at pH 4.0. As the pH continued to decrease, the R_h value also began to decrease, changing from 65.9 to 47.9 nm as the solution pH decreased from 4.0 to 3.0. This result indicates that the complex became more compact owing to further protonation of the pendant carboxylate groups in PMA. Figure 10b shows scattering intensities for the complex as a function of pH. The scattering intensity increased rapidly as the solution pH decreased from 4.9 to 4.0, suggesting that the complex was formed below pH 4.0. As the scattering intensity is proportional to the molecular mass, the observation that the scattering intensity was nearly constant between pH 4.0 and 3.0 suggests that the aggregation number of the complex was practically constant in this range.

CONCLUSIONS

The ABA triblock copolymer PSS-PEG-PSS was prepared via RAFT radical polymerization in water using a bifunctional PEG-based macro-chain transfer agent. The PMA homopolymer also underwent RAFT polymerization in water. Both polymerization reactions proceeded in accordance with a controlled mechanism. A mixture of

PSS-PEG-PSS and PMA formed a water-soluble complex in water at pH 3. The formation of the water-soluble complex was confirmed by ^1H NMR, light scattering, fluorescence probe and TEM techniques. ^1H NMR data indicated restricted motion of the PEG blocks in the complex owing to hydrogen bonding interactions between the PEG block and PMA. Light scattering and TEM data suggested that the PSS-PEG-PSS/PMA complex was spherical in shape. The CAC value of the complex was determined to be $\sim 0.06\text{ g l}^{-1}$ by DLS and fluorescence measurements. The complex dissociated to a unimer above pH 4.5.

ACKNOWLEDGEMENTS

This work was supported by a Grant-in-Aid (no. 23106717) for Scientific Research on Innovative Areas, 'Molecular Soft-Interface Science,' from the Ministry of Education, Culture, Sports, Science and Technology of Japan, which is gratefully acknowledged.

- Xu, R., Winnik, M. A., Riess, G., Chu, B. & Croucher, M. D. Micellization of polystyrene-poly(ethylene oxide) block copolymers in water. 5. A test of the star and mean-field models. *Macromolecules* **25**, 644–652 (1992).
- Harada, A. & Kataoka, K. Formation of polyion complex micelles in an aqueous milieu from a pair of oppositely-charged block copolymers with poly(ethylene glycol) segments. *Macromolecules* **28**, 5294–5299 (1995).
- Kabanov, V. A., Zezin, A. B., Kasaikin, V. A., Zakharova, J. A., Litmanovich, E. A. & Ileva, E. M. Self-assembly of ionic amphiphiles on polyelectrolyte chains. *Polym. Int.* **52**, 1566–1572 (2003).
- Foreman, M. B., Coffman, J. P., Murcia, M. J., Naumann, C. A., Cesana, S., Jordan, R., Smith, G. S. & Naumann, C. A. Gelation of amphiphilic lipopolymers at the air-water interface: 2D analogue to 3D gelation of colloidal systems with grafted polymer chains. *Langmuir* **19**, 326–332 (2003).
- Jeon, S. H. & Ree, T. Characterization of poly(carboxylic acid)/poly(ethylene oxide) blends formed through hydrogen bonding by spectroscopic and calorimetric analyses. *J. Polym. Sci. A* **26**, 1419–1428 (1988).
- Lee, W., Chang, J. & Ju, S. Hydrogen-bond structure at the interfaces between water/poly(methyl methacrylate), water/poly(methacrylic acid), and water/poly(2-aminoethyl-methacrylamide). *Langmuir* **26**, 12640–12647 (2010).
- Abe, K., Koide, M. & Tsuchida, E. Selective complexation of macromolecules. *Macromolecules* **10**, 1259–1264 (1977).
- Ikawa, T., Abe, K., Honda, K. & Tsuchida, E. Interpolymer complex between poly(ethylene oxide) and poly(carboxylic acid). *J. Polym. Sci. Polym. Chem. Ed.* **13**, 1505–1514 (1975).
- Koňák, Č. & Sedláček, M. pH-sensitive micelles formed by interchain hydrogen bonding of poly(methacrylic acid)-*block*-poly(ethylene oxide) copolymers. *Macromol. Chem. Phys.* **208**, 1893–1899 (2007).
- Holappa, S., Kantonen, L., Winnik, F. M. & Tenhu, H. Self-complexation of poly(ethylene oxide)-*block*-poly(methacrylic acid) studied by fluorescence spectroscopy. *Macromolecules* **37**, 7008–7018 (2004).
- Spijker, H. J., Dirks, A. J. & van Hest, J. C. M. Synthesis and assembly behavior of nucleobase-functionalized block copolymers. *J. Polym. Sci. Polym. Chem. Ed.* **44**, 4242–4250 (2006).
- Loxitz, B. S., Convertine, S. J., Ezwil, R. G., Heidenreich, A., Li, Y. & McCormick, C. L. Responsive nanoassemblies via interpolyelectrolyte complexation of amphiphilic block copolymer micelles. *Macromolecules* **39**, 8594–8602 (2006).
- Li, Y., Lokitz, B. S. & McCormick, C. L. Thermally responsive vesicles and their structural 'locking' through polyelectrolyte complex formation. *Angew. Chem. Int. Ed.* **45**, 5792–5795 (2006).
- Xu, X., Smith, A. E., Kirkland, S. E. & McCormick, C. L. Aqueous RAFT synthesis of pH-responsive triblock copolymer mPEO-PAPMA-PDPAEMA and formation of shell cross-linked micelles. *Macromolecules* **41**, 8429–8435 (2008).
- Mitsukami, Y., Donovan, M. S., Lowe, A. B. & McCormick, C. L. Water-soluble polymers. 81. Direct synthesis of hydrophilic styrenic-based homopolymers and block copolymers in aqueous solution via RAFT. *Macromolecules* **34**, 2248–2256 (2001).
- Achilleos, M., Legge, T. M., Perrier, S. & Patrickios, C. S. Poly(ethylene glycol)-based amphiphilic model conetworks: synthesis by RAFT polymerization and characterization. *J. Polym. Sci. A* **46**, 7556–7565 (2008).
- Pelet, J. M. & Putnam, D. High molecular weight poly(methacrylic acid) with narrow polydispersity by RAFT polymerization. *Macromolecules* **42**, 1494–1499 (2009).
- Meiboom, S. & Gill, D. Modified spin-echo method for measuring nuclear relaxation times. *Rev. Sci. Instrum.* **29**, 688–691 (1958).
- Meas, S. J., Cosgrove, T., Thompson, L. & Howell, I. Solvent relaxation NMR measurements on polymer, particle, surfactant systems. *Langmuir* **14**, 997–1001 (1998).
- Chu, B. *Laser Light Scattering: Basic Principle and Practice* 2nd edn (Academic Press, Boston, 1991).

- 21 Jakes, J. Regularized positive exponential sum (REPES) program—a way of inverting Laplace transform data obtained by dynamic light scattering. *Collect. Czech. Chem. Commun.* **60**, 1781–1797 (1985).
- 22 Brown, W., Nicolai, T., Hvidt, S. & Stepanek, P. Relaxation time distributions of entangled polymer solutions from dynamic light scattering and dynamic mechanical measurements. *Macromolecules* **23**, 357–359 (1990).
- 23 Stockmayer, W. H. & Schmidt, M. Effects of polydispersity, branching and chain stiffness on quasielastic light scattering. *Pure. Appl. Chem.* **54**, 407–414 (1982).
- 24 Phillies, G. D. J. Quasielastic light scattering. *Anal. Chem.* **62**, 1049A–1057A (1990).
- 25 Phillies, G. D. J. Upon the application of cumulant analysis to the interpretation of quasielastic light scattering spectra. *J. Chem. Phys.* **89**, 91–99 (1988).
- 26 Koppel, D. E. Analysis of macromolecular polydispersity in intensity correlation spectroscopy: the method of Cumulants. *J. Chem. Phys.* **57**, 4814–4820 (1972).
- 27 Donovan, M. S., Lowe, A. B., Sumerlin, B. S. & McCormick, C. L. RAFT polymerization of *N,N*-dimethylacrylamide utilizing novel chain transfer agents tailored for high reinitiation efficiency and structural control. *Macromolecules* **35**, 4123–4132 (2002).
- 28 Yusa, S., Fukuda, K., Yamamoto, T., Ishihara, K. & Morishima, Y. Synthesis of well-defined amphiphilic block copolymers having phospholipid polymer sequences as a novel biocompatible polymer micelle reagent. *Biomacromolecules* **6**, 663–670 (2005).
- 29 Yusa, S., Konishi, Y., Mitsukami, Y., Yamamoto, T. & Morishima, Y. pH-responsive micellization of amine-containing cationic diblock copolymers prepared by reversible addition-fragmentation chain transfer (RAFT) radical polymerization. *Polym. J.* **37**, 480–488 (2005).
- 30 Bain, A. D., Ho, W. P. Y. & Martin, J. S. A new way of measuring NMR spin–spin relaxation times (T_2). *J. Magn. Reson.* **43**, 328–330 (1981).
- 31 Matsukawa, S. & Ando, I. Study of self-diffusion of molecules in a polymer gel by pulsed-gradient spin-echo ^1H NMR. 2. Intermolecular hydrogen-bond interaction between the probe polymer and network polymer in *N,N*-dimethylacrylamide–acrylic acid copolymer gel systems. *Macromolecules* **30**, 8310–8313 (1997).
- 32 Xu, R., Winnik, M. A., Hallet, F. R., Riess, G. & Croucher, M. D. Light-scattering study of the association behavior of styrene-ethylene oxide block copolymers in aqueous solution. *Macromolecules* **24**, 87–93 (1991).
- 33 Slavik, J. Anilinoaphthalene sulfonate as a probe of membrane composition and function. *Biochim. Biophys. Acta.* **694**, 1–25 (1982).
- 34 Huber, K., Bantle, S., Lutz, P. & Burchard, W. Hydrodynamic and thermodynamic behavior of short-chain polystyrene in toluene and cyclohexane at 34.5 °C. *Macromolecules* **18**, 1461–1467 (1985).
- 35 Akcasu, A. Z. & Han, C. C. Molecular weight and temperature dependence of polymer dimensions in solution. *Macromolecules* **12**, 276–280 (1979).
- 36 Konishi, T., Yoshizaki, T. & Yamakawa, H. On the 'universal constants' ρ and Φ of flexible polymers. *Macromolecules* **24**, 5614–5622 (1991).
- 37 Yamamoto, Y., Nagasaki, Y., Kato, Y., Sugiyama, Y. & Kataoka, K. Long-circulating poly(ethylene glycol)–poly(D,L -lactide) block copolymer micelles with modulated surface charge. *J. Controlled Release* **77**, 27–38 (2001).
- 38 Tanford, C., Nozaki, Y. & Rohde, M. F. Size and shape of globular micelles formed in aqueous solution by *n*-alkyl polyoxyethylene ethers. *J. Phys. Chem.* **81**, 1555–1560 (1977).